



## First-Principles Prediction of Doped Graphane as a High-Temperature Electron-Phonon Superconductor

G. Savini,<sup>1,2</sup> A. C. Ferrari,<sup>1,\*</sup> and Feliciano Giustino<sup>3</sup>

<sup>1</sup>*Department of Engineering, University of Cambridge, Cambridge, CB3 0FA, United Kingdom*

<sup>2</sup>*Institute of Protein Research, University of Osaka, Osaka, 565-0871, Japan*

<sup>3</sup>*Department of Materials, University of Oxford, Oxford, OX1 3PH, United Kingdom*

(Received 11 March 2010; published 14 July 2010; corrected 15 July 2010)

We predict by first-principles calculations that *p*-doped graphane is an electron-phonon superconductor with a critical temperature above the boiling point of liquid nitrogen. The unique strength of the chemical bonds between carbon atoms and the large density of electronic states at the Fermi energy arising from the reduced dimensionality give rise to a giant Kohn anomaly in the optical phonon dispersions and push the superconducting critical temperature above 90 K. As evidence of graphane was recently reported, and doping of related materials such as graphene, diamond, and carbon nanostructures is well established, superconducting graphane may be feasible.

DOI: 10.1103/PhysRevLett.105.037002

PACS numbers: 74.10.+v, 63.22.Rc, 73.22.Pr, 74.20.Fg

The discovery of superconductors such as MgB<sub>2</sub> [1] and iron pnictides [2] intensified the search for high-temperature superconductivity in materials other than copper oxides. The critical temperature  $T_c$  reflects the energy scale of the interactions driving the condensation into the superconducting state. In high- $T_c$  copper oxides the nature of the interaction is still under debate, yet it is generally accepted that Coulomb exchange and correlation, with energy scales around few hundred meVs, play an important role [3,4]. In contrast, in conventional superconductors the pairing is driven by the electron-phonon interaction, with an energy scale of only a few ten meVs [5]. Because of the order-of-magnitude difference between such energy scales, it is assumed that conventional superconductors cannot exhibit  $T_c$  as high as copper oxides.

Here we show by density-functional theory (DFT) calculations that *p*-doped graphane may be a conventional superconductor with  $T_c$  well above the boiling point of liquid nitrogen. As evidence of graphane was recently reported [6,7], and doping of related materials such as graphene, diamond, and nanocarbons is well established, superconducting graphane may be feasible. Here we identify a conventional phonon-mediated superconducting pairing in close analogy to B-doped diamond [8].

The Bardeen-Cooper-Schrieffer (BCS) theory [5] defines the basic framework to understand conventional superconductivity. Its generalization, incorporating lattice dynamics, the Migdal-Eliashberg theory [9], provides a predictive computational tool. Within BCS,  $T_c$  is [5]

$$k_B T_c = 1.14 \hbar \omega_0 \exp(-1/N_F V), \quad (1)$$

where  $k_B$  is the Boltzmann constant,  $\hbar \omega_0$  a characteristic phonon energy,  $N_F$  the electronic density of states (EDOS) at the Fermi energy  $E_F$ , and  $V$  an effective pairing potential resulting from the net balance between the attractive electron-phonon coupling (EPC) and the repulsive electron-electron interaction [5]. Even though the original

BCS formula for  $T_c$  is now replaced by more refined expressions such as the modified McMillan equation [9], Eq. (1) still proves useful for discussing trends: One could maximize  $T_c$  by increasing the materials parameters  $\omega_0$ ,  $N_F$ , and  $V$ . However, these are strongly intertwined, making such optimization extremely complex. We now discuss a simple procedure, based on Eq. (1) and on recent advances in electron-phonon superconductivity, to design a novel high- $T_c$  superconductor.

Let us first consider the conventional superconductor with the highest  $T_c$ , MgB<sub>2</sub> ( $T_c = 39$  K) [1]. For simplicity, we neglect multiband and anisotropy effects [10,11]. In MgB<sub>2</sub> the EPC contribution to  $V$  is large ( $\sim 1.4$  eV, from  $\lambda = N_F V$ , using  $N_F = 0.7$  states/cell/eV, and  $\lambda \sim 1$  [11]) because the states with energy close to  $E_F$  (those which condensate in the superconducting state [5]) are of  $\sigma$  character, i.e., derive from bonding combinations of planar B  $sp^2$  hybrids localized around the middle of B—B bonds [10,11]. These are significantly affected by the B—B bond length variation associated with bond-stretching  $E_{2g}$  phonons [11], resulting in a large EPC contribution to  $V$ . At the same time, the energy of the  $E_{2g}$  phonons is large ( $\sim 60$  meV [11]), due to the small B mass, leading to a large  $\omega_0$  in Eq. (1). Furthermore, MgB<sub>2</sub> is a metal with a significant EDOS at  $E_F$  ( $\sim 0.7$  states/cell/eV [11]). These three factors cooperate to establish a superconducting state with  $T_c = 39$  K [10,11]. Experimental and theoretical attempts to improve upon MgB<sub>2</sub> by investigating related materials met limited success [12], with the experimental  $T_c$  never higher than MgB<sub>2</sub>.

We thus search for an alternative material having at least some of the desirable features of MgB<sub>2</sub>, i.e., (i)  $\sigma$  electrons at the Fermi surface, (ii) large bond-stretching phonon frequencies, and (iii) large EDOS at  $E_F$ . The first two requirements are met by B-doped diamond, a conventional BCS superconductor with  $T_c = 4$  K [8,13], where a small holelike Fermi surface appears around the top of the va-

lence band [14]. The electronic states at  $E_F$  have  $\sigma$  character deriving from bonding combinations of tetrahedral C  $sp^3$  hybrids, bearing some analogy to  $MgB_2$ . As these  $\sigma$  states are localized in the middle of the C—C bonds, they couple considerably to bond-stretching phonons [14,15], resulting in a large EPC contribution to  $V$ , even superior to  $MgB_2$  ( $\sim 3$  eV, from  $\lambda = N_F V$ , using  $N_F = 0.1$  states/cell/eV, and  $\lambda \sim 0.3$  [16]). In addition, the light C atoms have high energy optical phonons ( $\sim 130$  meV, even after softening induced by the large EPC [15,16]). However in B-doped diamond the EDOS at  $E_F$  is rather small ( $\sim 0.1$  states/cell/eV for 2% doping [14]), compromising  $T_c$ . While B-doped diamond shares some desirable features of  $MgB_2$ , its 3D nature implies the EDOS in proximity of the valence band scales as  $\sqrt{E}$  (with  $E$  from the valence band edge); see Fig. 1(a). Thus, the carriers available for the superconducting state are relatively few even for large doping. Superconducting diamond is then a 3D analogue of  $MgB_2$  [14,15].

The comparison between  $MgB_2$  and diamond leads to the question of what would happen in a hypothetical B-doped diamond with reduced dimensionality, such as a thin film or a nanowire, with the EDOS significantly enhanced by quantum confinement. The EDOS of a 2D semiconductor is a step function; hence, the number of available carriers can be large even at low doping. In order

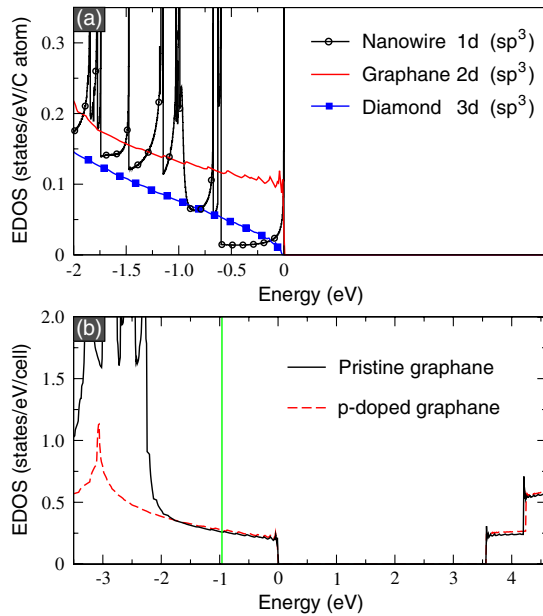


FIG. 1 (color online). (a) EDOS per carbon atom in 1D (diamond nanowire), 2D (graphane), and 3D (diamond). (b) EDOS of pristine (solid black line) and 12.5%  $p$ -doped graphane (dashed red line,  $2 \times 2$  supercell with one substitutional B). The top of the valence band is set as zero, and  $E_F = -0.96$  eV (green line). The EDOS at  $E_F$  is similar in the two models (0.26 states/eV/cell in rigid band; 0.27 states/eV/cell in supercell). We expect this to hold also at lower doping, where the perturbation to the pristine dispersions is smaller. The supercell calculation has no impurity states in the gap.

to estimate the EDOS increase in a diamond thin film, we consider a parabolic band model. For 2% B doping, bulk diamond has  $N_F = 0.1$  states/eV/cell at  $E_F$ . A 0.5-nm-thick diamond film with the same doping would have  $N_F \sim 0.5$  states/eV/cell. Such EDOS increase would significantly enhance  $T_c$ . With the electron-phonon potential and phonon frequency of bulk diamond, Eq. (1) gives that a 0.5-nm film would superconduct at  $T_c \sim 80$  K. This effect could be maximized by using an atomically thin diamond film. However, the question remains whether it is possible to synthesize such film.

Recent work on graphene and its derivatives points to a positive answer. Soon after the discovery of graphene [17], several works considered how to functionalize and chemically modify it [18–23]. In particular, it was proposed that fully hydrogenated graphene (graphane) would be stable [24]. The main difference between graphene and graphane is that, while the former is fully  $sp^2$  bonded, the latter is  $sp^3$ , as diamond [24]. Experimental evidence of graphane was recently reported [6,7]. Since graphane is the 2D counterpart of diamond, our scaling arguments point to doped graphane as a potential high- $T_c$  superconductor. Doping could be achieved by gating, including using an electrolyte gate, or by charge transfer, as done in graphene [18–20]. Substitutional doping of graphene was also reported, up to  $\sim 10^{14}$   $cm^{-2}$  [21].

We thus perform DFT calculations of EPC and  $T_c$  in doped graphane. By analogy with B-doped diamond, we consider  $p$  doping. We use the DFT local density approximation, plane waves, and pseudopotentials [25]. Hole doping is simulated within the rigid-band approximation. We checked that this is adequate to describe substitutional B doping by comparing the electronic structure with that of a supercell model explicitly including the B atoms [25]. Doping has the effect of lowering  $E_F$  below the top of the valence band and does not introduce localized states in the band gap. Phonon modes and EPCs are calculated within density-functional perturbation theory [26,27]. The EPCs,  $\lambda$ , are calculated by using a  $100 \times 100 \times 1$  grid. We extensively checked the convergence of  $\lambda$  with respect to Brillouin zone (BZ) sampling [25]. We calculate  $T_c$  by using the modified McMillan equation [9], together with a Coulomb parameter  $\mu^* = 0.13$ . Other Coulomb parameters do not affect our conclusions.

The  $p$ -doped graphane EDOS close to the valence band maximum follows a steplike behavior, as expected in 2D; see Fig. 1(b). At 3% doping this is 0.22 states/eV/cell, almost twice the 0.13 states/eV/cell of bulk diamond.

Figure 2 plots the phonon dispersions of pristine and  $p$ -doped graphane (see Ref. [25] for full dispersion); Fig. 3(a) plots the phonon density of states (PDOS). Upon doping, the optical zone-center modes associated with in-plane C-C stretching soften as a result of the inception of Kohn anomalies [28]. The softening of modes with large C-C stretching is similar to B-doped diamond [15,16]. The region of reciprocal space where the softening is observed matches the diameter  $2k_F$  of the hole Fermi surface around

$\Gamma$ , a typical signature of the Kohn effect [28]. The softening of the TO stretching modes ( $\sim 58$  meV or  $\sim 470$   $\text{cm}^{-1}$  at 1% doping) is significantly larger than the  $\sim 5$  meV of graphite and graphene [29]. The C-H stretching modes [25] do not soften and have negligible weight on EPC.

Figure 3(b) plots the Eliashberg spectral function [30], which shows the relative contribution of different modes to the superconducting pairing [30]:

$$\alpha^2 F(\omega) = \frac{1}{2} \sum_{\nu} \int_{BZ} \frac{d\mathbf{q}}{A_{BZ}} \omega_{\mathbf{q}\nu} \lambda_{\mathbf{q}\nu} \delta(\omega - \omega_{\mathbf{q}\nu}), \quad (2)$$

where  $\lambda_{\mathbf{q}\nu}$  is the EPC of mode  $\nu$  with momentum  $\mathbf{q}$  and frequency  $\omega_{\mathbf{q}\nu}$ ,  $\delta$  the Dirac delta, and  $A_{BZ}$  the BZ area. The TO in-plane C-C stretching phonons, with C and H moving in-phase [see Fig. 3(b) and Ref. [25]] have the largest EPC, due to the  $\sigma$  character of the states at  $E_F$  and the large C displacements, similar to B-doped diamond [14–16], validating our hypothesis that  $p$ -doped graphene can be seen as an ultrathin diamond.

Figure 4(a) plots EPC as a function of doping, and Fig. 4(b) the corresponding  $T_c$ . This exceeds the boiling point of liquid nitrogen and falls within the same range as copper oxides [31]. Because of the relatively constant EDOS [see Fig. 1(b)],  $T_c$  is rather insensitive to doping. This is important for the practical realization of superconducting graphene. Our results should be valid throughout the entire doping range considered here for gate- or charge-transfer-induced doping, since in these cases the holes are delocalized and are in the metallic regime. For substitutional doping we expect our results to apply beyond the metal-to-insulator transition (MIT). In the absence of experimental MIT measurements, the critical doping concentration can be estimated from a scaling argument as 5% B (1 B every 20 C) or  $2 \times 10^{14}$  holes  $\times \text{cm}^{-2}$  [25]. This could be feasible, considering that substitutional doping in graphene was reported up to 5% [21].

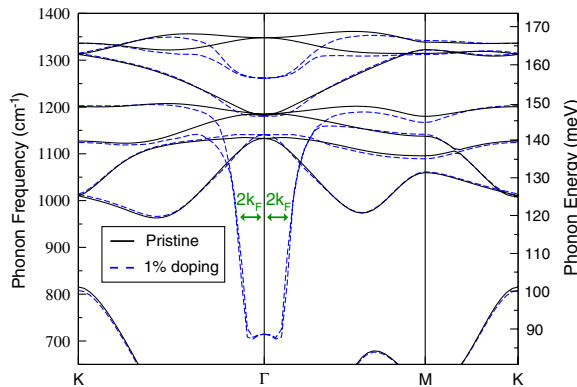


FIG. 2 (color online). Optical phonon dispersions of pristine (solid black line) and 1%  $p$ -doped graphene (dashed blue lines). The arrows indicate the average Fermi surface diameter, with the Kohn anomalies (see Ref. [25] for mode assignments). Calculations taking B explicitly into account [16] or with non-adiabatic corrections [39] may slightly revise the softening. However, this stands out as a qualitative effect.

Our findings bear consequences for both fundamental science and applications. One could envision hybrid superconducting or semiconducting circuits directly patterned through lithography, graphene-based Josephson junctions for nanoscale magnetic sensing, and ultimately an ideal workbench to explore the superconducting state in two dimensions [32]. The superconducting phase transition in graphene could also be controlled by gating [20,33], leading to novel switching mechanisms in nanoscale field-effect transistors. The superconducting mechanism identified here is expected to be valid even after including correlation effects beyond standard DFT. Indeed, GW bands of pristine graphene are in good agreement with DFT close to the valence band top [34].

The superconducting phase transition in systems with reduced dimensionality is the subject of numerous theoretical studies (see, e.g., Ref. [35]). Quantum fluctuations could destroy the superconducting order in 2D [36]. However, recent experiments suggest that this is not necessarily the case [32,33]. It was reported that the superconducting state in Pb is robust down to a single atomic layer [32,37]. Since our proposed mechanism is BCS-like, as in Pb, there should be no fundamental limits to superconducting graphene. We also expect partially hydrogen-

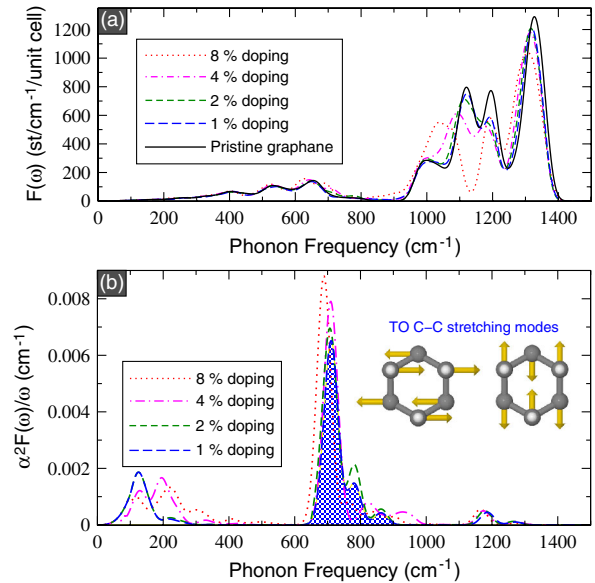


FIG. 3 (color online). (a) PDOS of pristine and  $p$ -doped graphene. (b) Eliashberg function for several dopings. We use Gaussians of width 2 meV to represent the Dirac deltas in the PDOS and Eliashberg functions. The largest EPC contribution arises from optical phonons, as in diamond [15], but also acoustic phonons couple to holes at the Fermi surface. The hashed region for 1% doping shows the TO stretching contributions to the Eliashberg function. (Inset) Ball-and-stick representations of two TO C-C stretching modes. The arrows indicate the displacement patterns (C atoms gray, H white). The in-plane C-C stretching modes with C and H out-of-phase do not contribute to EPC because, upon softening, the planar modes hybridize so that those at  $715$   $\text{cm}^{-1}$  have an increased weight on C atoms, the opposite of those at  $1257$   $\text{cm}^{-1}$ .

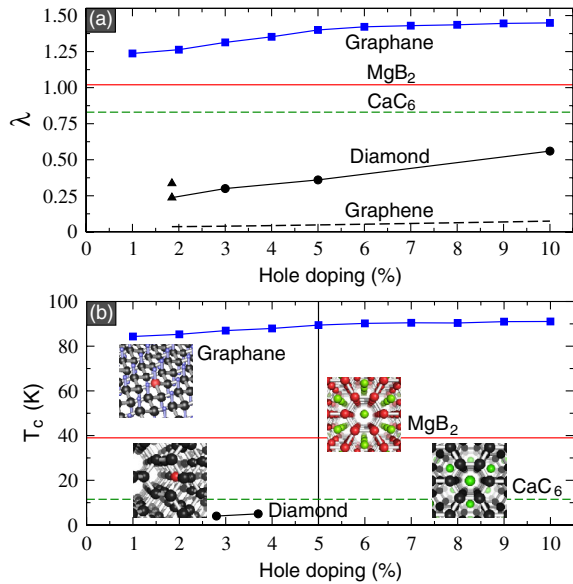


FIG. 4 (color online). (a) Total EPC in graphane and MgB<sub>2</sub> (solid red line [15]), CaC<sub>6</sub> (dashed green line [40]), diamond (solid black line [15]; triangles [16]), and graphene (dashed black line [41]). Note that EPC in graphene is small because the C atoms are  $sp^2$  and the states are  $\pi$  or  $\pi^*$  combinations of  $p_z$ , not coupling as much to in-plane C-C stretching [41]. (b)  $T_c$  from the modified McMillan formula with Coulomb pseudopotential  $\mu^* = 0.13$  [30]. The vertical black line indicates the doping corresponding to the estimated MIT. Below it, our formalism applies to charge transfer or gate-induced doping, while above it also applies to substitutional doping. For comparison, we show  $T_c$  of MgB<sub>2</sub> (solid red line,  $T_c = 39$  K [1]), CaC<sub>6</sub> (dashed green line,  $T_c = 11.5$  K [42]), and diamond (solid black line,  $T_c = 4$  K at  $\sim 2.8\%$  B [8]; 5 K at  $\sim 3.7\%$  B [43]). Taking explicitly into account a substitutional dopant, such as B, could slightly change the EPCs [16]. However, in B-doped diamond a rigid-band model provides lower EPC and lower bound to  $T_c$  [16]. Here we use the isotropic Eliashberg formalism [30]. Anisotropy may increase  $T_c$  [10]. (Inset) Ball-and-stick models of B-doped diamond, CaC<sub>6</sub>, MgB<sub>2</sub>, and B-doped graphane. C, black; H, blue; B, red; Mg, light green; Ca, green.

ated graphene to be superconducting, as the key elements are reduced dimensionality and  $sp^3$  bonds.

It is immediate to extend our results to diamond nanowires [38]. For a 1D system, the EDOS near a band edge has a van Hove singularity going as  $\sim 1/\sqrt{E}$ . Assuming phonon energies and EPC similar to graphane, Eq. (1) would yield  $T_c$  up to  $\sim 150$  K for a 1-nm nanowire [see EDOS in Fig. 1(a)]. The possibility of  $T_c$  higher than copper oxides by exploiting dimensionality deserves further investigation. Our work suggests that  $p$ -doped diamond nanostructures have an intriguing potential for high- $T_c$  BCS-like superconductivity.

We thank J. Noffsinger for useful discussions. Calculations were performed at HPCF (Cambridge) and the University of Ioannina using QUANTUM ESPRESSO. G. S. acknowledges funding from JSPS and Grant-in-Aid for

Scientific Research and A. C. F. from The Royal Society, the ERC grant NANOPOTS and EPSRC EP/G042357/1.

\*acf26@eng.cam.ac.uk

- [1] J. Nagamatsu *et al.*, *Nature (London)* **410**, 63 (2001).
- [2] Y. J. Kamihara *et al.*, *J. Am. Chem. Soc.* **130**, 3296 (2008).
- [3] P. W. Anderson, *Science* **316**, 1705 (2007).
- [4] T. A. Maier *et al.*, *Phys. Rev. Lett.* **100**, 237001 (2008).
- [5] J. Bardeen *et al.*, *Phys. Rev.* **108**, 1175 (1957).
- [6] D. C. Elias *et al.*, *Science* **323**, 610 (2009).
- [7] S. Ryu *et al.*, *Nano Lett.* **8**, 4597 (2008).
- [8] E. A. Ekimov *et al.*, *Nature (London)* **428**, 542 (2004).
- [9] P. B. Allen and B. Mitrovich, *Solid State Phys.* **37**, 1 (1983).
- [10] H. J. Choi *et al.*, *Nature (London)* **418**, 758 (2002).
- [11] J. M. An and W. E. Pickett, *Phys. Rev. Lett.* **86**, 4366 (2001).
- [12] H. J. Choi *et al.*, *Phys. Rev. B* **80**, 064503 (2009).
- [13] X. Blase *et al.*, *Nature Mater.* **8**, 375 (2009).
- [14] K. W. Lee and W. E. Pickett, *Phys. Rev. Lett.* **93**, 237003 (2004).
- [15] L. Boeri *et al.*, *Phys. Rev. Lett.* **93**, 237002 (2004).
- [16] F. Giustino *et al.*, *Phys. Rev. Lett.* **98**, 047005 (2007).
- [17] K. S. Novoselov *et al.*, *Proc. Natl. Acad. Sci. U.S.A.* **102**, 10451 (2005).
- [18] N. Jung *et al.*, *Nano Lett.* **9**, 4133 (2009).
- [19] I. Gierz *et al.*, *Nano Lett.* **8**, 4603 (2008).
- [20] A. Das *et al.*, *Nature Nanotech.* **3**, 210 (2008).
- [21] X. Wang *et al.*, *Science* **324**, 768 (2009).
- [22] T. Gokus *et al.*, *ACS Nano* **3**, 3963 (2009).
- [23] F. Cervantes-Sodi *et al.*, *Phys. Rev. B* **77**, 165427 (2008).
- [24] J. O. Sofo *et al.*, *Phys. Rev. B* **75**, 153401 (2007).
- [25] See supplementary material at <http://link.aps.org/supplemental/10.1103/PhysRevLett.105.037002> for technical details on the DFT calculations, the complete phonon dispersions and modes identification, and a discussion of the metal-to-insulator transition.
- [26] S. Baroni *et al.*, *Rev. Mod. Phys.* **73**, 515 (2001).
- [27] P. Giannozzi *et al.*, *J. Phys. Condens. Matter* **21**, 395502 (2009).
- [28] W. Kohn, *Phys. Rev. Lett.* **2**, 393 (1959).
- [29] S. Piscanec *et al.*, *Phys. Rev. Lett.* **93**, 185503 (2004).
- [30] G. Grimvall, *The Electron-Phonon Interaction in Metals* (North-Holland, New York, 1981).
- [31] W. E. Pickett, *Rev. Mod. Phys.* **61**, 433 (1989).
- [32] S. Qin *et al.*, *Science* **324**, 1314 (2009).
- [33] J. T. Ye *et al.*, *Nature Mater.* **9**, 125 (2010).
- [34] S. Lebegue *et al.*, *Phys. Rev. B* **79**, 245117 (2009).
- [35] T. M. Rice, *Phys. Rev.* **140**, A1889 (1965).
- [36] W. Skocpol and M. Tinkham, *Rep. Prog. Phys.* **38**, 1049 (1975).
- [37] T. Zhang *et al.*, *Nature Phys.* **6**, 104 (2010).
- [38] T. Yang *et al.*, *J. Chem. Phys.* **128**, 124709 (2008).
- [39] A. M. Saitta *et al.*, *Phys. Rev. Lett.* **100**, 226401 (2008).
- [40] M. Calandra and F. Mauri, *Phys. Rev. B* **74**, 094507 (2006).
- [41] C. H. Park *et al.*, *Nano Lett.* **8**, 4229 (2008).
- [42] N. Emery *et al.*, *Phys. Rev. Lett.* **95**, 087003 (2005).
- [43] K. Ishizaka *et al.*, *Phys. Rev. Lett.* **100**, 166402 (2008).